MNRAS 000, 1–8 (2015) Preprint 6 September 2016 Compiled using MNRAS LATEX style file v3.0

Power Spectrum Comparison... y ya veremos que mas!

O. Nicolás Gomez-Giraldo[1]⋆, Juan C. Muñoz-Cuartas†
[1]FACom - Instituto de Física, FCEN, Universidad de Antioquia UdeA, Calle 70 No. 52-21, Medellín, Colombia.

Accepted XXX. Received YYY; in original form ZZZ

ABSTRACT

Here we put the abstract

Key words: keyword1 – keyword2 – keyword3

Objetivo del paper: Mostrar las bondades de la estimación del bispectrum usando Daubechies. En particular mostrando los efectos del aliasing en el bispectrum.

1 INTRODUCTION

Presentación del problema. Resumen de la bibliografía. Qué es lo que hacemos. Por qué es importante. Esquleto del paper

Large Scale structure (LSS) of the Universe is thought to arise from the evolution of primordial fluctuations which are the result of gravitational instabilities at the early Universe (**cite**). In order to characterize quantitatively how is the clustering of these structures, different statistical methods are used to infer properties that can give constraints to cosmological models as well to cosmological parameters (**cite**). Because the statistical independence of the Fourier modes of a homogeneous random field, these statistics are expressed in Fourier space, which makes the study of such field easier (Martínez & Saar 2002).

The matter power spectrum is one of the most common statistical measures of gravitational clustering. Its importance arises from the fact that, for a gaussian random field, the power spectrum describes completely its statistical properties (**cite**). However, a complete description for a non-gaussian distribution, which can be primordial or can emerge from non-linear processes, requires the use of higher order correlation functions (Peebles 1980).

The bispectrum, had emerged as a standard probe of non-gaussianities in the LSS. The bispectrum is the lowest order indicator of non-Gaussinity in the primordial density field, which allows to constraint inflationary models and can give information about non-linear phenomena like structure formation and galaxy bias (**cite**). Despite its advantages, the estimation of the bispectrum is a task that is far from trivial. Due to its computational efficiency, it is common to use Fast Fourier Transforms in order to get different Fourier space statistics. Usually, computing power spectrum and bispectrum requires the interpolation of the density field in a cartesian grid. This interpolation is done via a mass assignment scheme (MAS), which is a convolution of the density field with a window function. The finite sampling of the convolved density field introduces an additional effect known as "aliasing", which is significant near to the Nyquist wavevector and has to be corrected for a precise estimation (Hockney & Eastwood 1981; Jing 2005; Jeong 2010).

Power spectrum had been measured from most of the redshifts survey, although, in the bispectrum case had been estimated in a lower amount **(dar ejemplos de estimaciones en otros papers)**.

In addition, power spectrum and bispectrum are also extensively estimated from N-body simulations. For this case, because of the large amount of particles involved, it is necessary to use fast Fourier transform (FFT) algorithms. Consequently, it is necessary to sample the density field $\rho(\mathbf{x})$ on a regular grid. This sampling process is mathematically equivalent to doing a convolution $\rho(\mathbf{x}_p) = [\rho * W](\mathbf{x}_p)$, where the function $w(\mathbf{x})$ is known as window function and its functional form depends on the way (scheme) used to sample the discrete particle distribution to the regular grid points. Therefore, the value obtained with FFT is not equal to the result obtained with Fourier transform (FT), in order to get the proper values it is necessary to correct the effects involved by the sampling on the regular grid (Jing 2005; Cui et al. 2008).

In this work we are going to study the impact of the MAS in the estimation of the bispectrum, mainly taking in account the aliasing effect.

poner estructura del articula

Qué es lo que se presenta nuevo en este trabajo? -> El impacto del MAS en $B(k_1 23)$.

⋆ E-mail: onicolas.gomez@udea.edu.co
† E-mail: jcmunozc@udea.edu.co

2 THEORY: POWER SPECTRUM, BISPECTRUM AND ESTIMATION

Teoría básica del $P(k)$ y $B(k1, k_2, k_3)$. Definiciones, estimadores (formalismo)

In cosmology, matter distribution is described as a continuous function of space and time. To study the properties related with these fields, statistical tools are used, mainly because there is not direct observational access to the cosmological fluctuations, furthermore, the involved scale times are so big that there is not possible to track the temporal evolution of a single system (Bernardeau et al. 2002; Martínez & Saar 2002).

Density fields had the properties of been statistically homogeneous and isotropic.

Knowledge of the distinct statistical properties at large scales can provide information about the nature of primordial overdensities, different possible inflationary scenarios, as well as give constrains on cosmological parameters and give information about different non linear phenomena such as gravity.

2.1 Power spectrum

The power spectrum $P(k)$ is the simplest Fourier statistic that allows to characterize the clustering pattern of the density field. It is the Fourier transform of the two point correlation function and can be defined from the density contrast in Fourier space $\delta(\mathbf{k}) = \int \exp(i\mathbf{k}\cdot\mathbf{r})\delta(\mathbf{r})\,\mathrm{d}^3\mathbf{r}$ as

$$\langle\delta(\mathbf{k}_1)\delta(\mathbf{k}_2)\rangle = (2\pi)^3\, P(k_1)\, \delta^D\,(\mathbf{k}_1 + \mathbf{k}_2) \tag{1}$$

where δ^D is the Dirac delta function and indicate the connected part between wavevectors $\mathbf{k}_1$ and $\mathbf{k}_2$, the symbol $\langle\cdots\rangle$ denotes the ensemble average over independent realizations of the Universe. Under the ergodicity hypothesis the average over different directions of the $\mathbf{k}$ will give the same result as the ensemble average (Gil-Marín et al. 2012).

For the density contrast field δ, the total variance can be written as

$$\sigma^2 = 4\pi \int_0^\infty P(k)\frac{k^2}{(2\pi)^3}\mathrm{d}k, \tag{2}$$

letting us to show an alternative form of the power spectrum also popular in cosmology

$$\Delta^2(k) = \frac{1}{2\pi}P(k)k^3, \tag{3}$$

accordingly, we can write the variance of the field as

$$\sigma^2 = \int_0^\infty \Delta^2(k)\mathrm{d}\,(\ln k)\,. \tag{4}$$

The power spectrum describes the second moment of a random field δ and represents an initial tool to characterize the clustering at large scales. For a Gaussian random field, the power spectrum describes completely its statistical features. The galaxy power spectrum had been extensively used in the literature to constraint structure formation, cosmological parameters as well as galaxy bias models, giving valuable information that helped to establish the ΛCDM as the standard cosmological model (Gil-Marín et al. 2012) **(Poner otras citas acá)**.

2.2 Bispectrum

When a random field is not Gaussian, is necessary to use higher order correlation functions in order the characterize the statistical properties of this field. The next statistic of interest is the bispectrum or the three point correlation function in Fourier space, which can be written as

$$\langle\delta(\mathbf{k}_1)\delta(\mathbf{k}_2)\delta(\mathbf{k}_3)\rangle = (2\pi)^3\,\delta^D\,(\mathbf{k}_1 + \mathbf{k}_2 + \mathbf{k}_3)\,B(k_1, k_2, k_3). \tag{5}$$

In this case, the Dirac delta function demands that the bispectrum is non-zero only for wavevector configurations that make closed triangles, i.e., $\mathbf{k}_1 + \mathbf{k}_2 + \mathbf{k}_3 = 0$. It is important to note that the product $\delta(\mathbf{k}_1)\delta(\mathbf{k}_2)\delta(\mathbf{k}_3)$ is in general a complex number, but once the mean is taken, the imaginary part goes to zero (Gil-Marín et al. 2012).

It is usual to define the reduced bispectrum Q by

$$Q(k_1,\, k_2,\, k_3) = \frac{B(k_1,\, k_2,\, k_3)}{P(k_1)P(k_2) + P(k_2)P(k_3) + P(k_3)P(k_1)}, \tag{6}$$

even this quantity does not give any additional information to the power spectrum and bispectrum it had been of historical used in cosmology because is the associated hierarchical amplitude for the bispectrum and is weakly dependent on cosmology and scale.

For a Gaussian random field bispectrum is null, therefore, it can be used as an initial tool to observe non-primordial Gaussinity. In addition, whether or not the random field is initially Gaussian or not, when non-linear processes (such as gravitational collapse) are present, they introduce non-gaussianities, allowing bispectrum to be used to extract information about non-linearities in the galaxy clustering. Besides, galaxy biasing also introduce non-linear effects in the density field, letting us to use bispectrum as an important tool to study galaxy bias at large scales (Matarrese et al. 1997; Gil-Marín et al. 2015).

2.3 Basic estimators

For the power spectrum the basic estimator is built by using direct sampling. This consists on taking the average of the complex magnitude of the density contrast in Fourier space in all the Fourier modes inside of a spherical shell of radius k and width $\Delta k = s\,k_F$, were $k_F = 2\pi/L$ is known as the fundamental frequency (for a comprehensive review of power spectrum and bispectrum estimation see Jeong (2010)). With this, the estimator is given by

$$P^d(k) = \frac{V_F}{(2\pi)^3}\left(\frac{1}{N_q}\sum_{k-\frac{\Delta k}{2}<|\mathbf{q}|<k+\frac{\Delta k}{2}} |\delta(\mathbf{q})|^2\right) \tag{7}$$

where N_k is the number of elements inside the selected shell and $V_F = k_F^3$.

The bispectrum estimator is given as the ensemble average of all the possible triangles with sides k_1, k_2, k_3. Therefore, the estimator is given as

$$B^d(k_1, k_2, k_3) = \frac{V_F}{(2\pi)^3}\left(\frac{1}{N_{\mathrm{Tri}}}\sum_{q\in \mathrm{Tri}_{123}} \delta(\mathbf{q}_1)\delta(\mathbf{q}_2)\delta(\mathbf{q}_3)\right) \tag{8}$$

where Tri_{123} is the set of points $\{\mathbf{q}_1, \mathbf{q}_2, \mathbf{q}_3\}$ satisfying simultaneously that its magnitude is $k_i - \Delta k/2 < |\mathbf{q}_i| < k_i + \Delta k/2$ and form a triangle, i.e., $\mathbf{q}_1 + \mathbf{q}_2 + \mathbf{q}_3 = \mathbf{0}$, N_{Tri} is the number of elements of Tri_{123}.

2.4 Shot noise

The shot noise is an additional term introduced as a consequence of the discrete sampling of the density field. Therefore, because of the discrete nature of the particle distribution in N-body simulations, it is necessary to correct the shot noise effect by substracting it from the power spectrum and bispectrum. The shot noise for the power spectrum and bispectrum is respectively

$$P_{SN}(k) = \frac{1}{\bar{n}}, \tag{9}$$

$$B_{SN}(k_1, k_2, k_3) = \frac{1}{\bar{n}}\left[P(k_1) + P(k_2) + P(k_3)\right] + \frac{1}{\bar{n}^2}, \tag{10}$$

where $\bar{n}$ is the number density of particles. Hence, the basic shot noise corrected estimators are given as

$$P(k) = P^d(k) - P_{SN}(k) \tag{11}$$

$$B(k_1, k_2, k_3) = B^d(k_1, k_2, k_3) - B_{SN}(k_1, k_2, k_3). \tag{12}$$

2.5 Mass assignment scheme: NGP, CIC, TGP, Deaubichis

Teoría básica del MAS. Definiciones, estimadores (formalismo). Implicaciones ventajas y desventajas de cada método.

For computational efficiency, statistics in Fourier space are usually calculated by making use of fast Fourier transform (FFT), in which is required a "sampling" on a regular grid of the overdensities values. From a practical standpoint this is equivalent to the convolution of the density contrast with a window function $W(\mathbf{k})$, defined by an assignation scheme [MAS; Hockney & Eastwood (1981)]. Once the overdensities in Fourier space are calculated power spectrum and bispectrum can measured through different estimators [*e.g.* Jeong (2010); Scoccimarro et al. (1998)].

The most common mass assignment schemes used are the Nearest Grid Point (NGP), Cloud In Cell (CIC) and Triangular Shaped Cloud (TSC), whith the window function given as $W(\mathbf{r}) = \prod_{i=1}^{3} W(x_i)$, where (Hockney & Eastwood 1981)

$$W_{NGP}(x) = \frac{1}{H}\begin{cases} 1 & \text{if } |x| < H/2 \\ 1/2 & \text{if } |x| = H/2 \\ 0 & \text{otherwise} \end{cases} \tag{13}$$

$$W_{CIC}(x) = \frac{1}{H}\begin{cases} 1 - |x|/H & \text{if } |x| < H \\ 0 & \text{otherwise} \end{cases} \tag{14}$$

$$W_{TSC}(x) = \frac{1}{H}\begin{cases} \frac{3}{4} - \left(\frac{x}{H}\right)^2 & \text{if } |x| \le \frac{H}{2} \\ \frac{1}{2}\left(\frac{3}{2} - \frac{|x|}{H}\right) & \text{if } \frac{H}{2} \le |x| \le \frac{3H}{2} \\ 0 & \text{otherwise,} \end{cases} \tag{15}$$

where H is the grid spacing. In addition, In the Figure 1 we plot the different forms of these window functions.

Given a wavevectors $\mathbf{k} = (k_1, k_2, k_3)$, the Fourier transform of the window functions for the different mass assignment schemes are given as a product of the Fourier transform

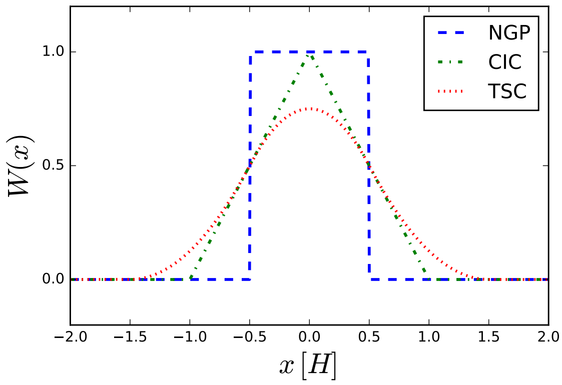

Figure 1. Graphic of the most common mass assignment schemes.

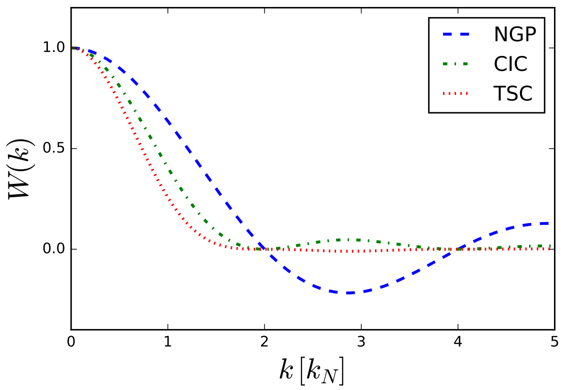

Figure 2. Graphic of the Fourier transform for the most common mass assignment schemes.

for each component

$$\begin{aligned} W(\mathbf{k}) &= \prod_{i=1}^{3} W(k_i) \\ &= \left[\prod_{i=1}^{3} \frac{\sin(\pi k_i/2k_N)}{\pi k_i/2k_N}\right]^p \end{aligned} \tag{16}$$

where $p = 1$ for NGP, $p = 2$ for CIC and $p = 3$ for TSC. In the Figure 2 we show the Fourier transform of the window functions in terms of k_N, we can see how for the NGP scheme it has appreciable values for values even bigger than $5k_N$ while in the CIC scheme for values $k \gtrsim 3k_N$ it drops and for the TSC when $k \gtrsim 2k_N$ it goes to zero.

(Figura: figurita con las formas!)

2.6 Aliasing for the power spectrum and bispectrum

In a practical sense, a mass assignment scheme is equivalent to a convolution of the density contrast with a window function (in which the particular form is defined by the scheme used). There is an effect introduced in the estimations of the power spectrum, bispectrum and their respective shot noise terms known as aliasing, which makes that the different modes in Fourier space lost its independence (Hockney & Eastwood 1981; Jing 2005).

Jing (2005) derived the power spectrum estimator when using FFT to get the desity constrast in Fourier space $\delta^f(\mathbf{k})$ as

$$\left\langle \left|\delta^f(\mathbf{k})\right|^2 \right\rangle = \sum_{\mathbf{n}} |W(\mathbf{k}+2k_N\mathbf{n})|^2 \, P(\mathbf{k}+2k_N\mathbf{n}) + \frac{1}{\bar{n}} \sum_{\mathbf{n}} |W(\mathbf{k}+2k_N\mathbf{n})|^2, \quad (17)$$

where $W(\mathbf{k})$ is the FT of the window function $W(\mathbf{r})$, $k_N = \pi/H$ is the Nyquist wavevectors and the summation is over the three dimensional integer vectors $\mathbf{n}$. Here we are going to deduce the alias effect but for the bispectrum.

By using FFT, the density contrast in Fourier space is given as (Jing 2005)

$$\delta^f(\mathbf{k}) = \frac{1}{\bar{n}} \sum_{\mathbf{g}} n^f(\mathbf{r}_g) \exp(i\mathbf{r}_g \cdot \mathbf{k}) - \delta^{\mathrm{K}}_{\mathbf{k},\mathbf{0}}, \quad (18)$$

where the superscript f means that the quantity was fast Fourier transformed, $n^f(\mathbf{r}_g)$ is the density convolved by the window function at the $\mathbf{g}$th grid point $\mathbf{r}_g = \mathbf{g}H$, here $\mathbf{g}$ is an integer vector,

$$n^f(\mathbf{r}_g) = \int n(\mathbf{r}) W(\mathbf{r}-\mathbf{r}_g) \, \mathrm{d}^3\mathbf{r}, \quad (19)$$

where δ^{K} is the Kronecker delta.

Equation (19) can be expressed in a different way by using the sampling function $\Pi(\mathbf{r})$ which is defined as

$$\Pi(\mathbf{r}) = \sum_{\mathbf{n}} \delta^D(\mathbf{r}-\mathbf{n}). \quad (20)$$

Defining a new convolved particle density

$$n'^f(\mathbf{r}) = \Pi\left(\frac{\mathbf{r}}{H}\right) \int n(\mathbf{r}_1) W(\mathbf{r}_1-\mathbf{r}) \, \mathrm{d}^3\mathbf{r}_1, \quad (21)$$

is possible to construct

$$\delta'^f(\mathbf{k}) = \frac{1}{\bar{n}} \int n'^f(\mathbf{r}) \exp(i\mathbf{r}\cdot\mathbf{k}) \, \mathrm{d}^3\mathbf{r} - \delta^{\mathrm{K}}_{\mathbf{k},\mathbf{0}}, \quad (22)$$

we have that (Jing 2005)

$$\delta'^f(\mathbf{k}) = \delta^f(\mathbf{k}), \quad (23)$$

therefore, the alternative form of equation (22) is

$$\delta^f(\mathbf{k}) = \frac{1}{\bar{n}} \int \Pi\left(\frac{\mathbf{r}}{H}\right) \sum_i n_i W(\mathbf{r}_i-\mathbf{r}) \exp(i\mathbf{r}\cdot\mathbf{k}) \, \mathrm{d}^3\mathbf{r} - \delta^{\mathrm{K}}_{\mathbf{k},\mathbf{0}}. \quad (24)$$

The three point ensemble average is given as

$$
\begin{aligned}
\langle\delta^f(\mathbf{k}_1)\delta^f(\mathbf{k}_2)\delta^f(\mathbf{k}_3)\rangle =& \frac{1}{\bar{n}^3}\int \Pi\left(\frac{\mathbf{r}_1}{H}\right)\Pi\left(\frac{\mathbf{r}_2}{H}\right)\Pi\left(\frac{\mathbf{r}_3}{H}\right)\\
&\times\left[\sum_{i\neq j\neq k}\langle n_i n_j n_k\rangle W(\mathbf{r}_{i1})W(\mathbf{r}_{j2})W(\mathbf{r}_{k3})\right.\\
&\left.+\sum_{i=j,i\neq k}\langle n_i^2 n_k\rangle W(\mathbf{r}_{i1})W(\mathbf{r}_{i2})W(\mathbf{r}_{k3})+\sum_{i=k,i\neq j}\langle n_i^2 n_j\rangle W(\mathbf{r}_{i1})W(\mathbf{r}_{j2})W(\mathbf{r}_{i3})+\sum_{j=k,i\neq j}\langle n_i n_j^2\rangle W(\mathbf{r}_{i1})W(\mathbf{r}_{j2})W(\mathbf{r}_{j3})\right]\\
&\times e^{i\mathbf{r}_1\cdot\mathbf{k}_1+i\mathbf{r}_2\cdot\mathbf{k}_2+i\mathbf{r}_3\cdot\mathbf{k}_3}\mathrm{d}^3\mathbf{r}_1\mathrm{d}^3\mathbf{r}_2\mathrm{d}^3\mathbf{r}_3\\
&-\frac{1}{\bar{n}^2}\int\Pi\left(\frac{\mathbf{r}_1}{H}\right)\Pi\left(\frac{\mathbf{r}_2}{H}\right)\left[\sum_{i\neq j}\langle n_i n_j\rangle W(\mathbf{r}_{i1})W(\mathbf{r}_{j2})+\sum_i\langle n_i^2\rangle W(\mathbf{r}_{i1})W(\mathbf{r}_{i2})\right]e^{i\mathbf{r}_1\cdot\mathbf{k}_1+i\mathbf{r}_2\cdot\mathbf{k}_2}\,\delta^K_{\mathbf{k}_3,\mathbf{0}}\,\mathrm{d}^3\mathbf{r}_1\mathrm{d}^3\mathbf{r}_2\\
&-\frac{1}{\bar{n}^2}\int\Pi\left(\frac{\mathbf{r}_1}{H}\right)\Pi\left(\frac{\mathbf{r}_3}{H}\right)\left[\sum_{i\neq k}\langle n_i n_k\rangle W(\mathbf{r}_{i1})W(\mathbf{r}_{k3})+\sum_i\langle n_i^2\rangle W(\mathbf{r}_{i1})W(\mathbf{r}_{i3})\right]e^{i\mathbf{r}_1\cdot\mathbf{k}_1+i\mathbf{r}_3\cdot\mathbf{k}_3}\,\delta^K_{\mathbf{k}_2,\mathbf{0}}\,\mathrm{d}^3\mathbf{r}_1\mathrm{d}^3\mathbf{r}_3\\
&-\frac{1}{\bar{n}^2}\int\Pi\left(\frac{\mathbf{r}_2}{H}\right)\Pi\left(\frac{\mathbf{r}_3}{H}\right)\left[\sum_{j\neq k}\langle n_j n_k\rangle W(\mathbf{r}_{j1})W(\mathbf{r}_{k3})+\sum_j\langle n_j^2\rangle W(\mathbf{r}_{j1})W(\mathbf{r}_{j3})\right]e^{i\mathbf{r}_2\cdot\mathbf{k}_2+i\mathbf{r}_3\cdot\mathbf{k}_3}\,\delta^K_{\mathbf{k}_1,\mathbf{0}}\,\mathrm{d}^3\mathbf{r}_2\mathrm{d}^3\mathbf{r}_3\\
&+\frac{1}{\bar{n}}\int\Pi\left(\frac{\mathbf{r}_1}{H}\right)\left[\sum_i\langle n_i^3\rangle W(\mathbf{r}_{i1})\right]e^{i\mathbf{r}_1\cdot\mathbf{k}_1}\,\delta^K_{\mathbf{k}_2,\mathbf{0}}\,\delta^K_{\mathbf{k}_3,\mathbf{0}}\,\mathrm{d}^3\mathbf{r}_1\\
&+\frac{1}{\bar{n}}\int\Pi\left(\frac{\mathbf{r}_2}{H}\right)\left[\sum_j\langle n_j^3\rangle W(\mathbf{r}_{j2})\right]e^{i\mathbf{r}_2\cdot\mathbf{k}_2}\,\delta^K_{\mathbf{k}_1,\mathbf{0}}\,\delta^K_{\mathbf{k}_3,\mathbf{0}}\,\mathrm{d}^3\mathbf{r}_2\\
&+\frac{1}{\bar{n}}\int\Pi\left(\frac{\mathbf{r}_3}{H}\right)\left[\sum_k\langle n_k^3\rangle W(\mathbf{r}_{k3})\right]e^{i\mathbf{r}_3\cdot\mathbf{k}_3}\,\delta^K_{\mathbf{k}_1,\mathbf{0}}\,\delta^K_{\mathbf{k}_2,\mathbf{0}}\,\mathrm{d}^3\mathbf{r}_3\\
&-\delta^K_{\mathbf{k}_1,\mathbf{0}}\,\delta^K_{\mathbf{k}_2,\mathbf{0}}\,\delta^K_{\mathbf{k}_3,\mathbf{0}},
\end{aligned}
\quad (25)
$$

where $\mathbf{r}_{ij} = \mathbf{r}_i - \mathbf{r}_j$. Taking volume intervals $\mathrm{d}V_i$ so small that the density number n_i is either 0 or 1, we have $n_i = n_i^2 = n_i^3 = \cdots$, $\langle n_i\rangle = \bar{n}\mathrm{d}V_i$, and for $\langle n_i n_j\rangle_{i\neq j} = \bar{n}^2\mathrm{d}V_i\mathrm{d}V_i\left[1+\langle\delta(\mathbf{r}_i)\delta(\mathbf{r}_j)\rangle\right]$ (Peebles 1980; Jing 2005). Also, using

$$
\Pi(\mathbf{k}) = \int \Pi\left(\frac{\mathbf{r}}{H}\right)e^{i\mathbf{r}\cdot\mathbf{k}}\mathrm{d}\mathbf{r} = \sum_{\mathbf{n}}\delta_{\mathbf{k},2k_N\mathbf{n}}, \quad (26)
$$

we get,

$$
\begin{aligned}
\langle\delta^f(\mathbf{k}_1)\delta^f(\mathbf{k}_2)\delta^f(\mathbf{k}_3)\rangle =& \sum_{\mathbf{n}_1,\mathbf{n}_2,\mathbf{n}_3}W(\mathbf{k'}_1)W(\mathbf{k'}_2)W(\mathbf{k'}_3)\left\langle\delta\left(\mathbf{k'}_1\right)\delta\left(\mathbf{k'}_2\right)\delta\left(\mathbf{k'}_3\right)\right\rangle\,\delta^K_{\mathbf{k'}_1+\mathbf{k'}_2+\mathbf{k'}_3,\mathbf{0}}\\
&+\frac{1}{\bar{n}}\sum_{\mathbf{n}_1,\mathbf{n}_2,\mathbf{n}_3}W(\mathbf{k'}_1)W(\mathbf{k'}_2)W(\mathbf{k'}_3)\left\langle\delta\left(\mathbf{k'}_1\right)\delta\left(\mathbf{k'}_2+\mathbf{k'}_3\right)\right\rangle\,\delta^K_{\mathbf{k'}_1+\mathbf{k'}_2+\mathbf{k'}_3,\mathbf{0}}\\
&+\frac{1}{\bar{n}}\sum_{\mathbf{n}_1,\mathbf{n}_2,\mathbf{n}_3}W(\mathbf{k'}_1)W(\mathbf{k'}_2)W(\mathbf{k'}_3)\left\langle\delta\left(\mathbf{k'}_2\right)\delta\left(\mathbf{k'}_1+\mathbf{k'}_3\right)\right\rangle\,\delta^K_{\mathbf{k'}_1+\mathbf{k'}_2+\mathbf{k'}_3,\mathbf{0}}\\
&+\frac{1}{\bar{n}}\sum_{\mathbf{n}_1,\mathbf{n}_2,\mathbf{n}_3}W(\mathbf{k'}_1)W(\mathbf{k'}_2)W(\mathbf{k'}_3)\left\langle\delta\left(\mathbf{k'}_3\right)\delta\left(\mathbf{k'}_1+\mathbf{k'}_2\right)\right\rangle\,\delta^K_{\mathbf{k'}_1+\mathbf{k'}_2+\mathbf{k'}_3,\mathbf{0}}\\
&+\frac{1}{\bar{n}^2}\sum_{\mathbf{n}_1,\mathbf{n}_2,\mathbf{n}_3}W(\mathbf{k'}_1)W(\mathbf{k'}_2)W(\mathbf{k'}_3)\,\delta^K_{\mathbf{k'}_1+\mathbf{k'}_2+\mathbf{k'}_3,\mathbf{0}}
\end{aligned}
\quad (27)
$$

For closed triangles we get

$$
\begin{aligned}
\left\langle\delta^f(\mathbf{k}_1)\delta^f(\mathbf{k}_2)\delta^f(\mathbf{k}_3)\right\rangle =& \sum_{\mathbf{n}_1,\mathbf{n}_2,\mathbf{n}_3}W(\mathbf{k'}_1)W(\mathbf{k'}_2)W(\mathbf{k'}_3)B(\mathbf{k'}_1,\mathbf{k'}_2,\mathbf{k'}_3)\\
&+\frac{1}{\bar{n}}\sum_{\mathbf{n}_1,\mathbf{n}_2,\mathbf{n}_3}W(\mathbf{k'}_1)W(\mathbf{k'}_2)W(\mathbf{k'}_3)\left[P(\mathbf{k'}_1)+P(\mathbf{k'}_2)+P(\mathbf{k'}_3)\right]\\
&+\frac{1}{\bar{n}^2}\sum_{\mathbf{n}_1,\mathbf{n}_2,\mathbf{n}_3}W(\mathbf{k'}_1)W(\mathbf{k'}_2)W(\mathbf{k'}_3)
\end{aligned}
\quad (28)
$$

Similar as (Jing 2005) explained for the case of power spectrum, equation (28) can be interpreted clearly. The convolution of the density contrast with the window function introduce a factor $W(\mathbf{k}_1)W(\mathbf{k}_2)W(\mathbf{k}_3)$ both to the bispectrum and its associated shotnoise $([P(k_1)+P(k_2)+P(k_3)]/\bar{n}+1/\bar{n}^2)$. As a consequence of the finite sampling of the convolved density contrast, we get an alias sum. The aliasing is particularly relevant close to the Nyquist wavevector k_N.

Teoría básica del aliasing. Definiciones, estimadores (formalismo). Implicaciones ventajas y desventajas de cada metodo. presentar Calculo del aliasing del aliasing general (nuevo?)
(Figura: Podemos hacer una grafica del formalismo "general" del aliasing comparando con lo que hay en el mercado)

3 METHODS

3.1 Simulation

The simulation we used to test the different scheme assignation consists on a cubic box of size $L = 400\,\mathrm{Mpc/h}$, with a particle number of $N_p = 512^3$ which was performed using the code GADGET. Initial conditions were generated using $\Omega_\Lambda = 0.742$, $\Omega_m = 0.258$, $\Omega_b = 0.0438$, $h = 0.72$, $n_s = 0.96$ and $\sigma_8(z = 0) = 0.796$.

In order to do the respective comparatives, we generated grids N_g of 64^3, 128^3, 256^3 and 512^3 cells where we used the NGP, CIC, TSC, D20 mass assignment schemes. For those grids we have that the fundamental wavevectors associated is $k_f = (2\pi)/L \approx 0.0157$ h/Mpc and that their Nyquist wavevector $k_N = (\pi N_g)/L$ are of 4.0212 h/Mpc, 2.0106 h/Mpc, 1.0053 h/Mpc, 0.5027 h/Mpc for the for the grids of 512^3, 256^3, 128^3, 64^3 cells respectively. It is important to take in account that the value of the Nyquist wavevector for the grid of 512^3 cells is eigth times larger than the grid of 64^3 cells. This is going to be an important fact later on because we are goint to use this argument to compare bispectrum results with different grids to analyze how is the alaising effect for the difference schemes used in this paper.

Describir los datos de las simulaciones, por que? pa' que?

3.2 Power spectrum estimation

To estimate power spectrum we first we choose a particular mass assignment scheme, which can be the NGP, CIC, TSC, and the Daubechies scale function D20. From a given number of grids, we spread the mass to the nearby cells according to a window function (which functional form depends of the MAS selected). Once the mass assignment scheme is done we took the Fourier transform of the density contrast by using the FFTW3 library (Frigo & Johnson 2005). Then, for a given wavevector magnitude value k, in order to fulfill the estimator given in (7), we first selected all the density contrast values whose associated wavevector $\mathbf{q}$ have a magnitude between the range $k - \frac{\Delta k}{2}$ to $k + \frac{\Delta k}{2}$ and got the mean of their square magnitude by summing and then dividing by the number of elements on the grid in the selected range N_q. Later, for the aliasing correction, similarly to Montesano et al. (2010) and Jeong & Komatsu (2009), we divided during the summation each $|\delta(\mathbf{q})|^2$ term in (7) by $\sum_{\mathbf{n}} |W(\mathbf{q} + 2k_N\mathbf{n})|^2$ which, according to the scheme used, is taken as (Jing 2005; Cui et al. 2008)

$$\sum_{\mathbf{n}} |W(\mathbf{k}')|^2 = \begin{cases} 1 & \text{NGP} \\ \prod_{i=0}^{3}\left[1 - \frac{2}{3}\sin^2\left(\frac{\pi k_i}{2k_N}\right)\right] & \text{CIC} \\ \prod_{i=0}^{3}\left[1 - \sin^2\left(\frac{\pi k_i}{2k_N}\right) + \frac{2}{15}\sin^4\left(\frac{\pi k_i}{2k_N}\right)\right] & \text{TSC} \\ 1 & \text{D20,} \end{cases} \tag{29}$$

whith $\mathbf{k}' = \mathbf{k} + 2k_N\mathbf{n}$. When the mean of the squared magnitude of the density contrast is taken, we multiply by the normalization constant $V_F/(2\pi)^3$ and finally we subtract the shotnoise term given in (9).

3.3 Bispectrum estimation

The steps involved in the bispectrum estimation are similar to the power spectrum case. For this, we use the estimator given in (8) in which we selected the triplets $\delta(\mathbf{k}_1)\delta(\mathbf{k}_2)\delta(\mathbf{k}_3)$ if their corresponding wavevectors met the condition of forming a triangle, i.e., $\mathbf{k}_1 + \mathbf{k}_2 + \mathbf{k}_3 = 0$. In order to do this, we selected first the set of points $\mathbf{q}_1$ and $\mathbf{q}_2$ which are in the range $k_i - \frac{\Delta k}{2}$ to $k_i + \frac{\Delta k}{2}$, for $i = 1, 2$. Then, $\mathbf{q}_3$ points are searched with the triangle constraint (i.e., that $\mathbf{q}_1$, $\mathbf{q}_2$ and $\mathbf{q}_3$ must form a triangle) then we select the points which are in the range $k_3 - \frac{\Delta k}{2}$ to $k_3 + \frac{\Delta k}{2}$. Sadly, this searching strategy can be a very computationally expensive process, because its order of computation of $O(N^2)$, so we have to search for other ways to improve the search. For this, we found one in which, taking in account the fact that $\delta(\mathbf{x})$ is a real value, we used the property $\delta(-\mathbf{k}) = \delta^*(\mathbf{k})$, letting us to use only one semiplane and being four time faster than the original strategy. For the aliasing correction, during the summation we divided each triplet by the product of the window functions $W(\mathbf{k}_1)W(\mathbf{k}_2)W(\mathbf{k}_3)$, were $W(\mathbf{k}_i) = W(k_{i,x})W(k_{i,y})W(k_{i,z})$. We multiply the normalization constants in (8) and finally we subtract the shotnoise term given in (10).

3.4 Aliasing effect

The alias sum introduce an effect in which the values that are outside of the Nyquist wavevector is falsely moved inside the range. Therefore, any wavevector component out of the Nyquist wavevector is aliased, i.e., spuriously moved into the range due to the discrete sampling (Press et al. 1992).

In order to measure the effect of the aliasing in the power spectrum and bispectrum, we are going to use the feature that for wavevector magnitudes close to the inside Nyquist wavevector the aliasing effect is particularly relevant, while for wavevector magnitudes with $k \ll k_N$ the aliasing effect is negligible. Hence, if we compare two estimations, one in which the aliasing is negligible at a given range (e.g. if we choose a grid with a number of cells big enough), and we compare with one in which the aliasing effect is high, we can get a way to compare the aliasing for different mass assignment schemes. We are going to use this approach for this work.

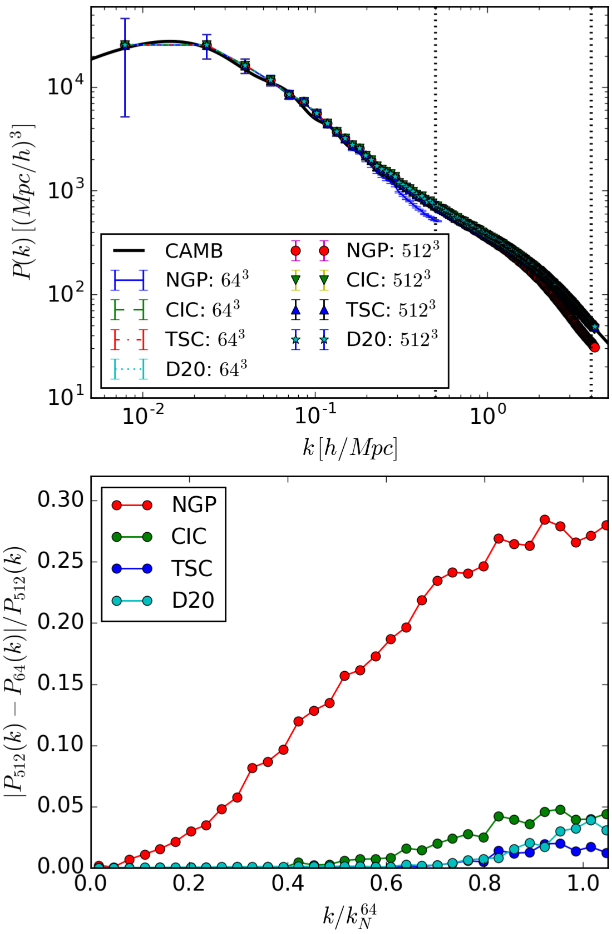

Figure 3. Graphic of the Fourier transform for the most common mass assignment schemes.

Como se estima el espectro de potencia y bispectrum en los datos? detalles de la implementacion. Pruebas? Todo funciona bien? -> comparaciones con el modelo teorico! Una buena descripcion para dummies de como calcular el bispectrum.

4 RESULTS

4.1 Power spectrum

In the Figure 3, in the upper panel we show the power spectrum estimation using the different schemes of this work for the grids of 512^3 and 64^3 cells against the result modeled with CAMB under the same cosmological parameters. As we can see, the values of the power spectrum are, in general, compatible the CAMB values. In the lower panel we show the percentage difference for the different schemes with respect the cells with 512^3 and 64^3 cells. For the NGP scheme we can get deviation of the order of 27% at the k_N level whereas for the CIC, TSC and D20 schemes we have deviations of 4%, 1.5% and 3.5%, respectively, therefore, the best results are obtained these three MAS.

(**Qué más digo???... No tengo una idea muy clara de cómo enfocarlo**)

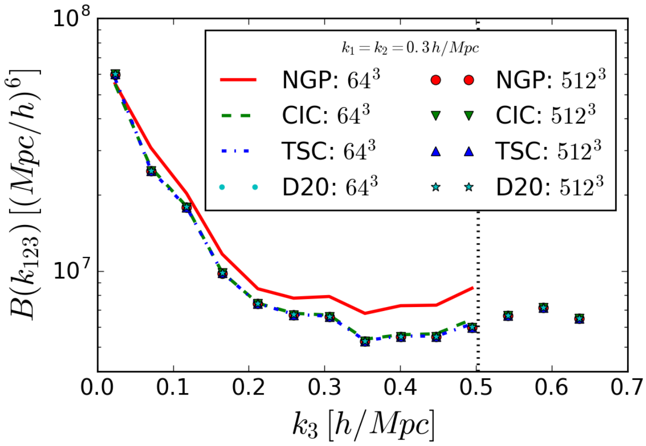

Figure 4. The aliasing effect in the power spectrum estimation for the most common schemes.

Discutir el resultado de Pk con los diferentes MAS (Colombi et.al. 2009). Efectos del aliasing, shot noise y demas. Como va eso en el Bk? (figura: Pk con los diferentes MAS, mascas de kf, etc)

4.2 Bispectrum

In the Figure 4 we show the results of the bispectrum for the grids of 512^3 and 64^3 cells. For the grid of 64^3 we have a good match between the different values estimated, except for the case in which the NGP scheme was used, meaning this that is not really useful to use this type of MAS for the bispectrum estimation. For the other MAS we have instead that while the wavevector get closer to the Nyquist value there is a deviation that not exceed the 5% difference.

In the upper panel of the Figure 5 we show how is the percentual difference for the MAS with respect to their distance to the Nyquist value when the alias correction in the bispectrum is not made but the shotnoise term is substracted. As we can see, the D20 scheme has the best match with the "non-aliased" result but as k_3 side is getting closer to k_N it can reach a percentual difference of 30%. In the lower panel we show the bispectrum estimation after aliasing and shotnoise correction. As we can see after corrections the results improves except for the NGP scheme and getting the best results for the D20 and TSC schemes, were for the D20 scheme can reach a percentual difference of 1% at the k_N level.

Así nos dio el bispectrum comparación del bispectrum con los diferentes MAS. Analisis de diferencias. (figura: Bk con los diferentes MAS, mascas de kf, etc)

4.3 Aliasing

Estimar (cuantitativaente) los efectos del aliasing (Figura: estimacion del aliasing, variaciones fraccionales, etc)

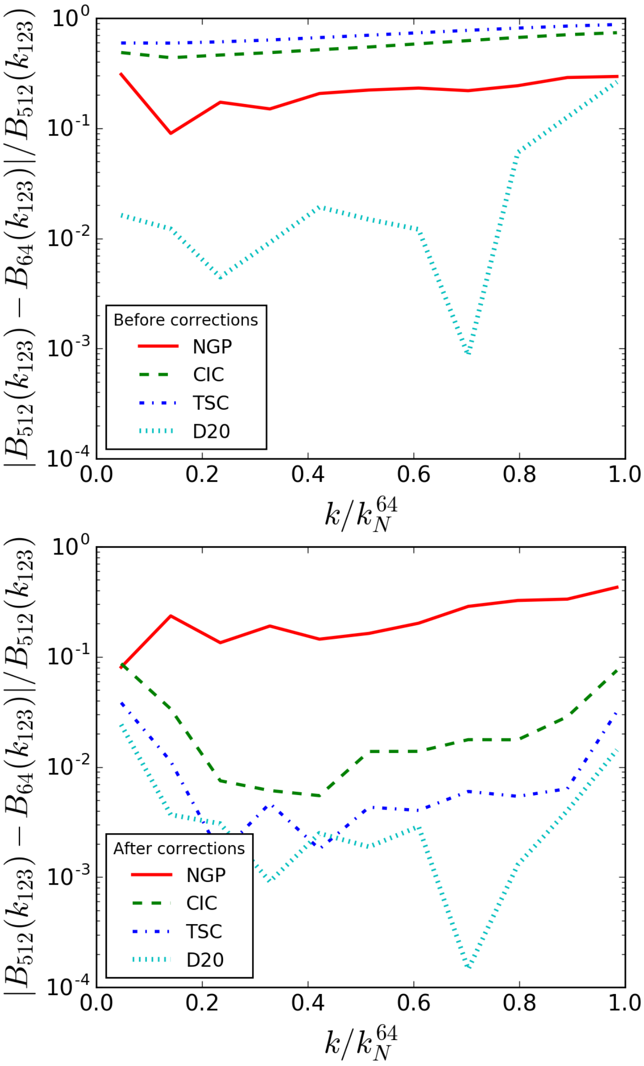

Figure 5. The aliasing effect in the power spectrum estimation for the most common schemes.

5 SUMMARY AND DISCUSSION

In this work we use numerical simulations to study the effect of the MAS in the estimation of power spectrum and bispectrum. The effect of the aliasing on the power spectrum and bispectrum is estimated numerically in order to measure its impact on the final statistics. We show comparisons of different MAS in the power spectrum and bispectrum and conclude that using the standard cloud in cell method results in a biased bispectrum (close to 8%) for values close the Nyquist wavevector. On the other hand, the triangular shaped cloud and Daubechies scaling function schemes show the best performance with the minimum aliasing effect with relative small deviations (3% and 1% respectively). We found that a MAS in the form of a Daubechies wavelet scaling function produces a very small aliasing effect on the bispectrum.

Finally, we present an analytic form for the aliasing of the bispectrum independent of the MAS that in general provides a way to estimate the effect of aliasing on bispectrum estimates. This result is important, since in the current age of percent precision cosmology, accurate estimators of power spectrum and bispectrum are a mandatory tool to probe the cosmic mass density field. It is worth to mention that this is one of the first works studying systematically this effect on the bispectrum.

ACKNOWLEDGEMENTS

The Acknowledgements section is not numbered. Here you can thank helpful colleagues, acknowledge funding agencies, telescopes and facilities used etc. Try to keep it short.

REFERENCES

Bernardeau F., Colombi S., Gaztañaga E., Scoccimarro R., 2002, Physics Reports, 367, 1
Cui W., Liu L., Yang X., Wang Y., Feng L., Springel V., 2008, ApJ, 687, 738
Frigo M., Johnson S. G., 2005, Proceedings of the IEEE, 93, 216
Gil-Marín H., Wagner C., Fragkoudi F., Jimenez R., Verde L., 2012, Journal of Cosmology and Astroparticle Physics, 2, 047
Gil-Marín H., Noreña J., Verde L., Percival W. J., Wagner C., Manera M., Schneider D. P., 2015, Monthly Notices of the Royal Astronomical Society, 451, 539
Hockney R. W., Eastwood J. W., 1981, Computer Simulation Using Particles
Jeong D., 2010, PhD thesis, University of Texas at Austin
Jeong D., Komatsu E., 2009, ApJ, 691, 569
Jing Y. P., 2005, Astrophysical Journal, 620, 559
Martínez V. J., Saar E., 2002, Statistics of the Galaxy Distribution. Chapman & Hall/CRC
Matarrese S., Verde L., Heavens A. F., 1997, Monthly Notices of the Royal Astronomical Society, 290, 651
Montesano F., Sánchez A. G., Phleps S., 2010, MNRAS, 408, 2397
Peebles P. J. E., 1980, The large-scale structure of the universe. Addison-Wesley, Princeton, N.J.
Press W. H., Teukolsky S. A., Vetterling W. T., Flannery B. P., 1992, Numerical recipes in C. The art of scientific computing
Scoccimarro R., Colombi S., Fry J. N., Frieman J. A., Hivon E., Melott A., 1998, ApJ, 496, 586

APPENDIX A: SOME EXTRA MATERIAL

If you want to present additional material which would interrupt the flow of the main paper, it can be placed in an Appendix which appears after the list of references.

This paper has been typeset from a TEX/LATEX file prepared by the author.